2023 IEEE International Symposium on Antennas and Propagation and USNC-URSI Radio Science Meeting (USNC-URSI) | 978-1-6654-4228-2/23/$31.00 ©2023 IEEE | DOI: 10.1109/USNC-URSI52151.2023.10238249

Vanadium Dioxide Aperture-Coupled mmWave 1–bit Reconfigurable Dual Polarization Reflectarray

Walter Disharoon and Nima Ghalichechian
Georgia Institute of Technology, Atlanta, GA 30332, USA, (wdisharoon3@gatech.edu, nima.1@gatech.edu)

Abstract— **A vanadium dioxide aperture-coupled patch 1-bit reconfigurable reflectarray was designed for operation in the n260 5G Band (37–40 GHz). The reflectarray can be used with a dual linearly polarized feed. The unit cell was simulated with a periodic boundary condition. The maximum reflection loss in the unit cell is less than 2 dB for both polarizations. The phase difference is 180° between the bits at the center frequency. Fabrication progress and finite array simulations will be presented at the conference.**

I. Introduction

With the expansion of use of frequency bands in mmWave to THz, there is a requirement for low-cost high-gain, and steerable antennas to overcome the significant path loss. Typical beamforming approaches can be used to steer the beam, but phased arrays introduce lossy, complex feed networks and expensive electronics. Reconfigurable reflectarrays (RRAs) are a low-cost, low-profile solution that removes the need for complex feed networks making RRAs an ideal option for mmWave communication for 5G and 6G. Typically the reconfigurability for reflectarrays has been implemented using diodes, but diode methods introduce far too much loss in the mmWave band [1]. Recently our group has investigated using both vanadium dioxide (VO_2) [2] and mechanical approaches for reconfiguration [3]. The unit cell for the VO_2 RRA had very low loss, but the final design was hampered by low aperture efficiency due to the high-permittivity sapphire substrate.

VO_2 is a metal-insulator-transition material which behaves like a high resistivity insulator ($\sigma = 80\, S/m$) when below 68°C, and as a conductor ($\sigma = 377000\, S/m$) otherwise. The major factor prohibiting the use of VO_2 in radiating structures is that the material has only been shown to maintain this high contrast ratio when deposited on high-permittivity materials such as silicon and sapphire [4]. This work builds upon previous aperture-coupled patch reflectarrays [5], [6] to take advantage of the high-permittivity substrates in this architecture, and the wideband, low-loss nature of VO_2 switches. In this work we discuss the design and simulation results for an aperture-coupled mmWave VO_2 RRA.

II. Design

The stackup for the unit cell is shown in Fig. 1(a). The top PCB has a low permittivity to allow for better radiation performance and higher aperture efficiency. The middle substrate uses a high permittivity to have a smaller delay line, allow deposition of VO_2, and reduce back radiation. Finally, the optional bottom substrate and back plate is used to entirely stop back radiation. The top-down view of the vertical layers is shown in Fig. 1(b–d). The parameters utilized are summarized in Table I. The width of the patch W_p is set at the center of resonance and the length of the slot L_s is optimized to cancel out the resonance allowing for a more linear-phase coupling to the delay line. The stub length is then tuned to the value that maintains a linear phase curve with the lowest loss. Finally, the length of the delay line L_d is set to allow for a 180° phase shift at the center frequency of the n260 5G band (37–40 GHz). The width of the copper line can also be tuned because a 50 Ω line is not a requirement for a reflectarray. By canceling out the resonance, a smaller reflection loss and more wideband phase curve can be achieved.

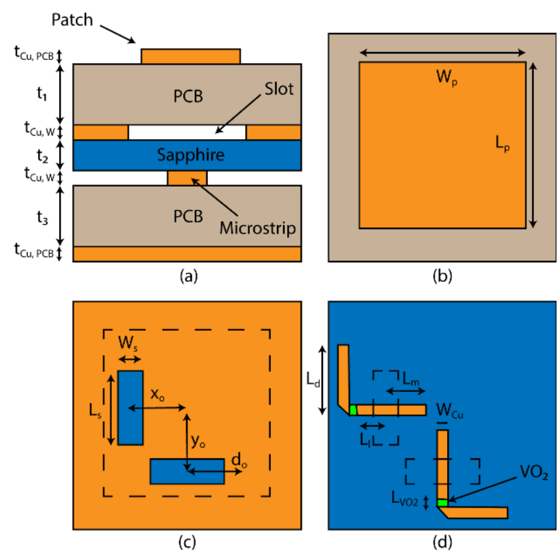

Fig. 1. (a) The stackup of the antenna. (b) The top-down view of the patch layer. (c) the top-down view of the slot layer. (d) The top-down view of the delay line layer. The dashed line shows the important feature from the above layer for visualizing alignment. The copper is orange and the VO_2 is in green.

TABLE I. Design Parameters

Parameter	Value	Parameter	Value
t_1	0.508 mm	$W_p = L_p$	2 mm
t_2	0.100 mm	W_s	0.14 mm
t_3	0.508 mm	L_s	1.5 mm
$t_{Cu,\ W}$	0.800 µm	W_{cu}	50 µm
$t_{Cu,\ PCB}$	17.5 µm	d_o	0.7 mm
t_{VO2}	0.100 µm	L_l	0.35 mm
L_d	1.25 mm	L_{VO2}	30 µm
L_m	0.35 mm	W_{VO2}	50 µm
x_o	0.7 mm	y_o	0.7 mm
ϵ_{pcb}	2.1	ϵ_{saph}	9.4

By having two orthogonal slots, dual linear polarization or circular polarization feeds can be supported. If using a dual pol design, the slots and delay lines need to be offset from the center to maximize the distance between the stubs and avoid cross-pol coupling between the two modes. The slots and lines are offset from the center by d_o.

III. Results

The design was simulated using a unit-cell Floquet port simulation in CST Studio. The simulated unit cell phase performance can be seen in Fig. 2, while the reflectivity performance can be seen in Fig. 3. the phase difference is 180° at 38.5 GHz, while the reflectivity remains above −2 dB for the *x*- and *y*-polarized incident wave. The cross-pol for the unit cell is below -10 dB in the band of operation for all switch cases. The electric field around the patch, in the slot, and around the line is shown in Fig. 4 for the *x*-polarized incident wave. The reflection loss is higher than our previous VO_2 RRA by 1.6 dB [2], but the aperture efficiency is expected to be higher due to the radiating structure not being placed on the high-permittivity substrate. Even with the higher loss than our previous design, the loss is respectably lower than comparable mmWave RRAs. A comparison between unit cells is shown in Table II. Fabrication progress and finite array simulations will be presented at the conference.

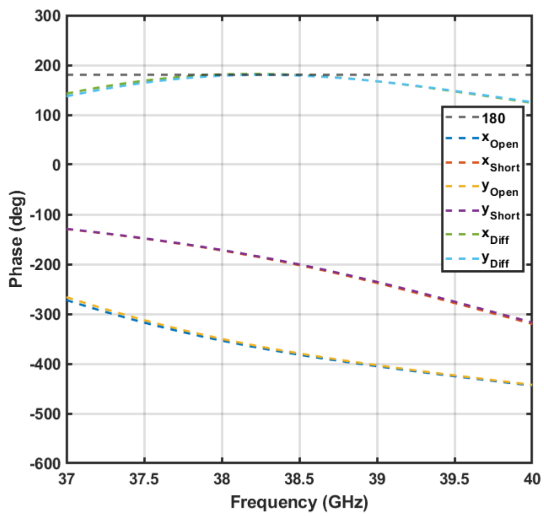

Fig. 2. The phase difference for both polarization is 180° at 38.5 GHz. Short and open refers to the state of the VO_2 switch in the delay line path.

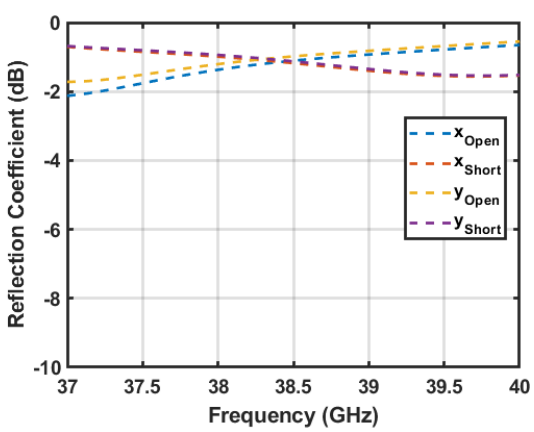

Fig. 3. The reflectivity for the x-pol and y-pol input for the two states is above −2 dB. Short and open refers to the state of the VO_2 switch in the delay line path

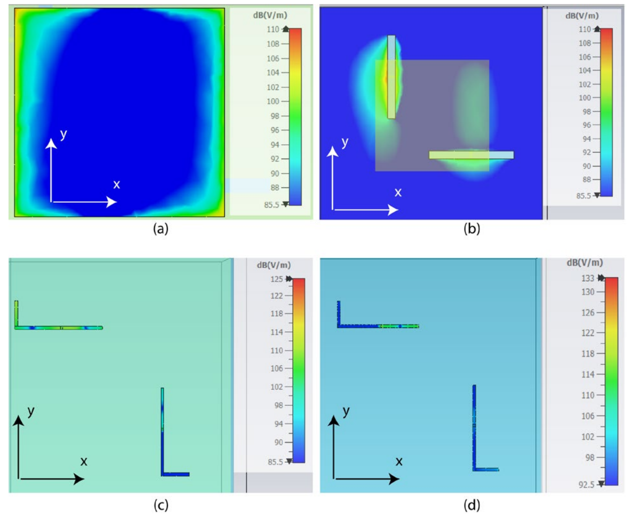

Fig. 4. Maximum electric field distribution on the (a) patch, (b) slot, (c) delay line for the short circuit case with an *x*-polarized incident wave, and (d) delay line for the open circuit case. The field hits the largest peak in the delay line.

TABLE II. Unit Cell Comparison

Reference	**This work (Sim)**	**[2]**	**[7]**
f_0	38.5 GHz	35 GHz	31.6 GHz
$\lvert S_{11}\rvert$	$> -2\ dB$	$> -0.4\ dB$	$> -7.5\ dB$
Phase Range	180° (1–bit)	180° (1–bit)	240° (cont)

References

[1] S. V. Hum and J. Perruisseau-Carrier, “Reconfigurable Reflectarrays and Array Lenses for Dynamic Antenna Beam Control: A Review,” *IEEE Trans. Antennas Propag.*, vol. 62, no. 1, 2014.

[2] J. Ramsey, K. Henderson, and N. Ghalichechian, “Thermally Actuated Vanadium Dioxide Millimeter Wave Reflectarray,” in *2022 16th European Conference on Antennas and Propagation (EuCAP)*, Mar. 2022, pp. 1–3.

[3] K. Q. Henderson, N. Ghalichechian, and W. Disharoon, “Mechanically Reconfigured Reflectarray Using Tunable Height Dielectric,” IEEE Trans. Antennas Propag. (In Press).

[4] M. Lust, S. Chen, C. E. Wilson, J. Argo, V. Doan-Nguyen, and N. Ghalichechian, “High-contrast, highly textured VO2 thin films integrated on silicon substrates using annealed Al2O3 buffer layers,” *J Appl Phys*, vol. 127, 205303 vols., 2020.

[5] E. Carrasco, M. Barba, and J. A. Encinar, “Reflectarray Element Based on Aperture-Coupled Patches With Slots and Lines of Variable Length,” *IEEE Trans. Antennas Propag.*, vol. 55, no. 3, 2007.

[6] E. Carrasco, M. Barba, B. Reig, C. Dieppedale, and J. A. Encinar, “Characterization of a Reflectarray Gathered Element With Electronic Control Using Ohmic RF MEMS and Patches Aperture-Coupled to a Delay Line,” *IEEE Trans. Antennas Propag.*, vol. 60, no. 9, pp. 4190–4201, Sep. 2012.

[7] K. K. Karnati, M. E. Trampler, and X. Gong, “A Monolithically BST-Integrated K_a -Band Beamsteerable Reflectarray Antenna,” *IEEE Trans. Antennas Propag.*, vol. 65, no. 1, Jan. 2017.